-RESEARCH PAPER-

International Journal of Mining and Geo-Engineering

IJMGE`

IJMGE 59-3 (2025) 221-228

DOI: 10.22059/IJMGE.2025.368129.595122

Shear behavior at the interface: experimental study on the roles of sand grain size and concrete surface roughness

Allahkaram Janipour [a], Mohsen Mousivand [b], Meysam Bayat [a,*]

[a] *Department of Civil Engineering, Najafabad Branch, Islamic Azad University, Najafabad, Iran.*

[b] *Department of Civil Engineering, Gonbad Kavoos Branch, Islamic Azad University, Gonbad Kavoos, Iran.*

Article History:

Received: 14 November 2023.

Revised: 28 February 2025.

Accepted: 19 May 2025.

ABSTRACT

This study provides novel insights into the shear resistance behavior at the concrete-sand interface, focusing on the combined effects of sand grain size, concrete surface roughness, and soil relative density. While individual parameters have been explored in previous research, this work systematically examines their interactions to better understand interface shear strength. A series of large direct shear tests was conducted on concrete-sand samples with varying surface roughness values (R_{max} = 0, 0.2, 4, and 8 mm) and granular materials with different mean particle sizes (D_{50} = 0.25 mm, 0.8 mm, and 2 mm). The granular materials were compacted to different relative densities (D_r = 30%, 60%, and 90%). The results revealed that increasing relative density from 30% to 60%, and from 30% to 90%, led to substantial rises in interface friction (approximately 105% and 306%, respectively). Coarser sand exhibited a more pronounced increase in interface friction angle than finer sand. Furthermore, increasing concrete surface roughness from 2 mm to 8 mm resulted in a 27% increase in the friction angle. These findings highlight the significant role of these parameters in governing the interaction between concrete and granular soil, offering valuable insights for applications in civil engineering.

Keywords: *Sand, Concrete, Interface, Relative density, Interface.*

1. Introduction

In various civil engineering projects, the interaction between different materials, such as foundations, piles, soil, and concrete, plays a crucial role in determining the stability and performance of structures, including the load-bearing capacity, settlement behavior, and long-term durability of geotechnical systems [1,2]. Previous research has highlighted that the static and seismic responses of materials are significantly influenced by interface characteristics [3–6]. While some earlier studies assumed the rigidity of interfaces and neglected interface parameters [7,8], others approximated these parameters as constant values [9]. However, recent findings underscore the potential errors introduced by such assumptions [10–13], emphasizing the need to consider various factors affected by interface parameters, including material characteristics and soil type.

Although surface roughness is typically described as a continuous variation in texture, it can also be represented by discrete surface modifications such as grooves or asperities. In this study, the height of the grooves was used as a parameter to quantify roughness, as it influences the mechanical interlocking between sand and concrete.

Surface roughness has been identified as a significant factor influencing interface parameters in previous studies [14–20]. Kishida and Uesugi [21] introduced the roughness coefficient for steel, and Gokhale and Drury [22] extended this concept to formulate the surface roughness of materials such as wood and concrete. Chen et al. [16] employed a new roughness definition to reveal three distinct phases of the friction angle in clay-concrete interfaces. Hu and Pu [14] conducted direct shear tests using modified samples, presenting critical relative roughness values for smooth and rough surfaces. Additionally, Hamid and Miller [15] explored the influence of matric suction and normal stress on steel-clay interfaces, demonstrating direct effects on soft and rough interfaces. Han et al. [12] investigated the effects of steel roughness with random directions, sand shape, and size on interface shear parameters, revealing that smaller sand size led to a higher friction angle, while the surface roughness of steel also contributed to an increase. Ahmadi et al. [23] investigated the mobilized shear strength at the interface between silica and calcareous sands and concrete and steel surfaces. Their results indicated that the mobilized shear strength was primarily influenced by factors such as relative density, surface roughness, sand type, and the type of material (steel or concrete).

Furthermore, Su et al. [24] found that greater structural material roughness resulted in a higher interface friction angle. Studies employing direct shear tests have investigated the effects of various parameters on cohesive soils and other material interfaces, determining cohesion and friction angle values [25,26]. Notably, previous research has highlighted the role of steel surface corrosion in altering cohesion and friction angle at the interface [27–29]. However, as many studies considered irregular roughness types, and since the specific manner of their distribution on object surfaces remains unknown, their findings may not provide sufficient insight into the effects of interface parameters.

The grain size curves of soils also exert a significant impact on interface shear behavior, with studies focusing on both cohesive and non-cohesive soils [30–32]. Uesugi and Kishida [31] explored the friction angle of dry sand-steel interfaces using direct shear, emphasizing the importance of particle size. Athanasopoulos [32] reported test results evaluating the interface behavior between sand and geotextile, revealing the influential effect of sand particle size on the

* Corresponding author: *E-mail address:* bayat.m@iaun.ac.ir (M. Bayat).

interface friction angle. Su et al. [24] confirmed that the particle size of sand primarily affects the interface friction angle. Wang et al. [26] studied the effects of grouting and surface roughness on clay-concrete interfaces, highlighting that grouting only influenced interface cohesion, with no impact on the friction angle. Similar results were found in other studies [30,33].

To date, no comprehensive study has been conducted to investigate the combined effects of concrete surface roughness and sand particle size on interface characteristics. This work addresses this gap by examining the interface between sand and concrete with varying concrete roughness, sand particle size, and relative density.

2. Experimental procedure

2.1. Materials

2.1.1. Sand

In this study, three types of sands, namely fine, medium, and coarse sands, were employed to explore the influence of particle size on interface parameters, as illustrated in Figure 1. The sands exhibited a nearly uniform composition. Particle size distribution tests were conducted according to the ASTM D422 standard, and the grading curves of the sands are presented in Figure 2. Table 1 provides additional characteristics of the sands utilized in this research.

Table 1. Geotechnical characteristics of the sands.

Characteristics	Fine Sand	Medium Sand	Coarse Sand
G_s (-)	2.71	2.72	2.72
D_{10} (mm)	0.14	0.32	1
D_{30} (mm)	0.2	0.52	1.4
D_{50} (mm)	0.25	0.8	2
D_{60} (mm)	0.3	1	2.5
C_u (-)	2.14	3.13	2.5
C_c (-)	0.95	0.85	0.78
e_{min}	0.54	0.45	0.42
e_{max}	0.91	0.81	0.79
MDD (g/cm^3)	1.91	1.92	1.93
OMC (%)	8	7	7
Soil Type (UCSC)	SP	SP	SP

Figure 1. Sands used in this research.

2.1.2. Cement

To produce concrete blocks, Type II cement (PO42.5) was utilized, and its physical characteristics are detailed in Table 2.

2.1.3. Concrete blocks

In this study, concrete blocks with varying degrees of roughness were employed. The concrete samples were fabricated using fine-grained silica sand and Type II cement with a consistent mixing ratio (sand, cement, and water in a ratio of 1.8,3,1, respectively).

2.2. Direct shear test

A large-scale shear test, featuring dimensions of 300×300×140 mm, was conducted in this study. Concrete blocks were prepared in accordance with ASTM C31, measuring 300×300×70 mm in size. Following the molding process, the concrete was allowed to cure for a period of 28 days. The height of the concrete specimen was precisely aligned with the shear line boundary, as illustrated in Figure 3, showcasing the preparation of the sample for interface analysis. Figure 4 demonstrates that the grooves and shear load direction were perpendicular.

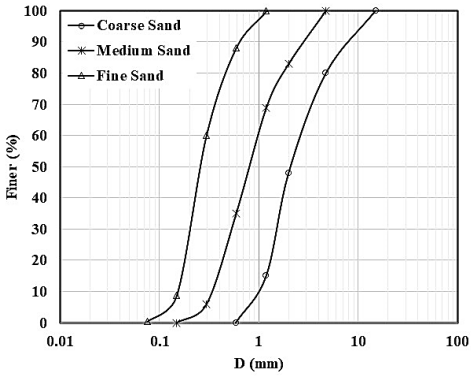

Figure 2. Grading curves of the sands.

Table 2. Physical and chemical properties of the cement.

Property/composition	Value
Specific gravity	3.14
Specific surface area (m2/kg)	320
Water demand (%)	32
Start of setting (min)	170
End of setting (min)	215
Compressive strength at 2 days (MPa)	41
Tensile strength at 2 days (MPa)	6.7
CaO (%)	60.4
SiO_2 (%)	15.9
Al_2O_3 (%)	9.5
SO	6.4
Fe_2O_3 (%)	4.1
MgO (%)	0.9
K_2O (%)	0.7
TiO_2 (%)	0.1

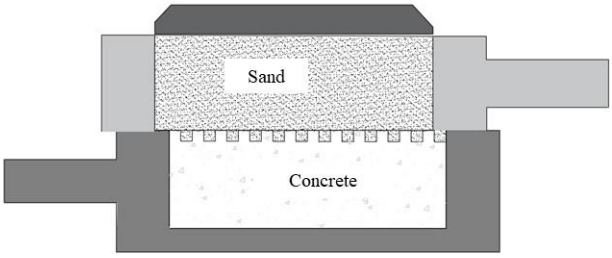

Figure 3. Preparation of the sample for interface study.

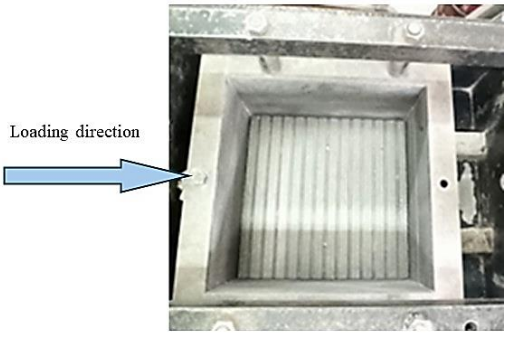

Figure 4. Direction of grooves and shear load.

As depicted in Figure 5, four concrete samples were employed in the study, each featuring a different R_{max} (0, 2, 4, and 8 mm). A customized mold was crafted specifically for the production of these concrete samples. To achieve this, four distinct molds with varying groove depths and a constant groove width of 10 mm were created. These grooves were formed on the bottom of the mold, and after pouring the concrete, they resulted in grooves with the desired depth on the concrete bottom surface.

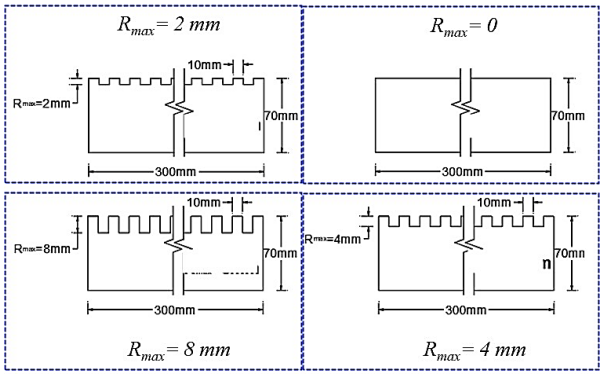

Figure 5. Concrete samples with different Rmax values.

2.3. Test procedure

In the experimental investigation of soil-concrete interaction, distinct sand types were thoughtfully selected and processed in their dry state. The chosen sand underwent a transformative process by spending 24 hours in a 105°C oven. Following adaptation, the direct shear sample was meticulously prepared. A concrete plate was placed at the base of the direct shear apparatus. Sand, prepared to the required relative density, was then added to the mold for testing. With precision, a specific quantity of sand, tailored to its relative density, was carefully introduced into the mold, primed for its role in the forthcoming tests. In this study, different relative densities were achieved by precisely measuring the volume of the upper section of the mold, including the grooves filled with sand. Based on the target relative density and the specific sand properties (i.e., maximum and minimum void ratios, R_{max} and R_{min}), the required weight of sand was calculated. This predetermined amount of sand was then placed into the mold and compacted to achieve the specified height.

Upon settling and deliberate compaction of the sand, a specialized cover for the shear box descended onto the granular stage, bearing the weight of anticipation. The conductor of forces, represented by normal stress, entered the scene, applying measured pressure to the awaiting sands. The performance unfolded with three distinguished guests: normal stress values of 50, 100, and 200 kPa, each taking their turn in the spotlight. As the stage was arranged and the sands faced pressure, the time came for the shear load to step in a controlled displacement on the granular surface. This displacement followed the cadence of ASTM D3080 standards, progressing at a deliberate speed of 1 mm/min. As the shear load was applied, the vertical load remained constant throughout the test. The sands, subjected to this orchestrated duet of forces, were tested at varying relative densities of 30%, 60%, and 90% with each revealing a distinctive response to the experiment's choreography.

3. Results

This study focuses on investigating the impact of several parameters, including sand grain size, concrete surface roughness, and relative density, on the interface between sand and concrete. To achieve this objective, a series of direct shear tests were conducted, and the findings are presented as follows:

3.1. Pure sand

To scrutinize the impact of relative density on shear strength parameters, a careful orchestration of tests unfolded. Coarse-grained sand, with a D_{50} of 2mm, took center stage, experiencing the limelight at different relative densities—30%, 60%, and 90%. Across this spectrum, the stage was set with three distinct normal stress values (50, 100, and 200 kPa). The results of these meticulously conducted direct shear tests are artfully presented in Figure 6. In the visual language of data, Figure 6 encapsulates the culmination of these experiments, offering a snapshot of the shear strength parameters as they respond to the intricate interplay of relative density and normal stress. Figure 6 unveils a clear trend where an elevation in both normal stress and relative density is associated with a notable increase in shear strength. This observation highlights the interconnected influence of these two factors, showcasing their substantial impact on shaping shear strength parameters.

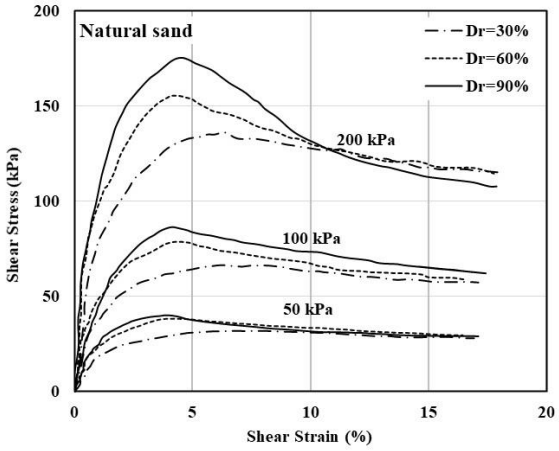

Figure 6. Shear stress- shear strain curves of course-grained sand specimens under different relative densities.

To delve deeper into the nuanced dynamics, a comprehensive set of direct shear tests was undertaken. This involved the examination of three distinct sands, each characterized by varying sizes (D_{50}=0.25, 0.8, and 2mm). The primary aim was to scrutinize how grading characteristics influence the shear strength parameters of sand. These direct shear tests were meticulously executed, maintaining a consistent relative density of 60%. The outcome of these tests is meticulously documented and visualized in Figure 7.

Figure 7 presents a visual representation, offering insights into the shear behavior across a range of sand sizes. This exploration not only enriches our understanding of the intricate relationship between grading characteristics and shear strength but also contributes to the broader comprehension of the complex interplay governing the behavior of sand interfaces.

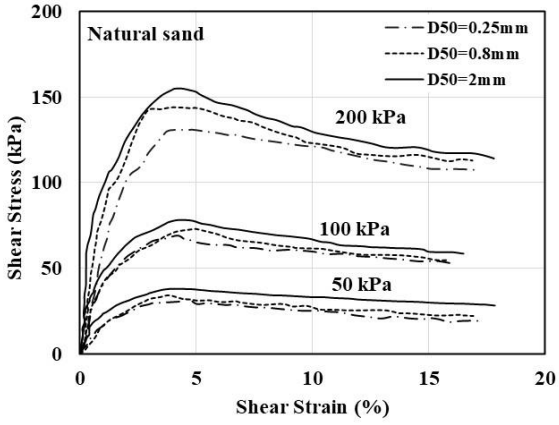

Figure 7. Shear stress- shear strain curves of fine, medium, and coarse sands under relative density 60%.

As illustrated, the elevation of the mean effective size of sand, transitioning from 0.25 to 2 mm, corresponds to an escalation in shear strength. Specifically, with incremental increases in the mean effective size, such as from 0.25 mm to 0.8 mm and 0.8 mm to 2 mm, the shear strength experiences an increment of 8% and 18%, respectively. This trend can be attributed to the increased inter-particle contact area and enhanced mechanical interlocking as the grain size increases. Larger sand grains typically have a rougher surface texture, leading to more effective particle-to-particle friction at the interface. Additionally, larger grains tend to form a more stable and interlocking structure, reducing the likelihood of particle slippage under applied stress. The increased frictional resistance from larger grains can be attributed to their ability to form more robust contact points and resist displacement under shear forces. In contrast, finer sands tend to have a lower shear strength due to their smaller particle size, which results in less interlocking and lower frictional resistance at the interface.

Figure 8 intricately portrays the fluctuation in shear strength ratio, denoting the ratio of shear strength concerning different sand grain sizes to that of fine sand (D_{50} = 0.25mm). This depiction provides a visual insight into the relative changes in shear strength across varying sand grain sizes, underscoring the significant impact of mean effective size on the overall shear strength characteristics. As shown in Figure 8, there is no consistent trend for the variation of shear strength ratio with normal stress level and D_{50}. In general, the samples with D_{50} = 0.8 mm exhibit higher values of shear strength ratio compared to those with D_{50} = 2 mm.

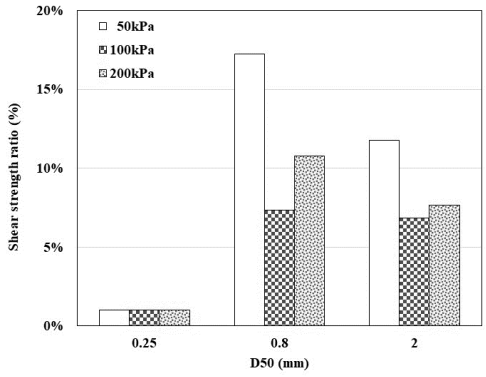

Figure 8. Variation of shear strength ratio.

Evidently, the size of the grains plays a significant role in determining soil shear strength. In instances of a constant grain size, such as D_{50}= 0.8mm, a noteworthy pattern emerges. With an increase in normal stress from 50 to 100 kPa, there is a reduction in shear stress by approximately 15%. However, further elevating the normal stress from 100 to 200 kPa results in a substantial increase in shear stress, amounting to approximately 92%. This trend is similarly observed in the context of a larger grain size, specifically 2 mm.

To visualize the impact of grain size on shear strength, Figure 9 presents the direct shear strength envelopes of coarse-grained sand (D_{50} = 2mm) across three distinct relative densities (30%, 60%, and 90%). This comprehensive representation offers a visual narrative of the intricate relationship between grain size, relative density, and shear strength, shedding light on the dynamic interplay within the soil matrix.

As evident, an increase in relative density corresponds to a rise in the sand friction angle. Across varying relative densities (30%, 60%, and 90%) the corresponding friction angle values are approximately 35, 37, and 41 degrees, respectively. This observation emphasizes the direct relationship between relative density and the frictional resistance of the sand.

Figure 10 illustrates the friction angle ratio, serving as an indicator of the percentage increase, across different relative densities. This graphic depiction offers a clear insight into the proportional changes in friction angle as relative density varies, underscoring the influence of soil compaction on the frictional characteristics of the sand.

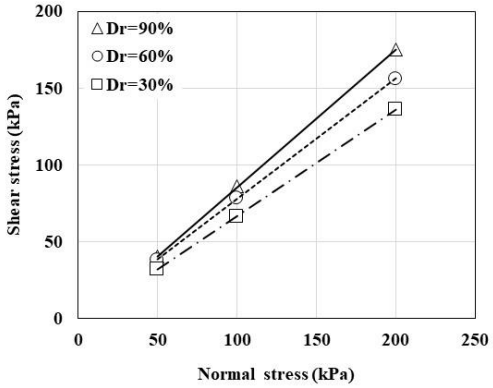

Figure 9. Direct shear strength envelopes of coarse sand (D50 =2mm) with different relative densities (Dr =30, 60, and 90%)

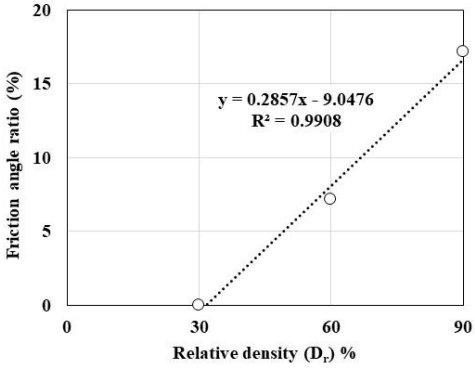

Figure 10. Friction angle ratio in different relative densities.

The presented findings underscore a clear linear relationship between relative density and friction angle. The incremental increase in relative density from 30 to 60 and 90, corresponds to a proportional increase in the friction angle, measuring approximately 7% and 17%, respectively. This linear trend aligns seamlessly with the observations from other studies, as illustrated in Figure 11. Notably, the diagrams from Chen et al. [34] and Maghvan et al. [35] showcase a parallel pattern, reinforcing the consistency and agreement across multiple investigations. This congruence strengthens the reliability and validity of the observed relationship between relative density and friction angle in the current study.

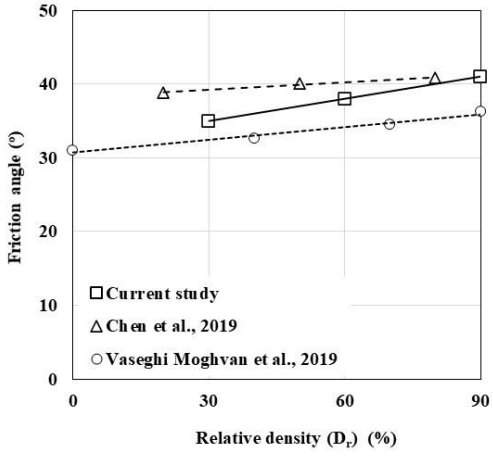

Figure 11. Effect of relative density on the friction angle.

Examining the outcomes, it becomes evident that a linear relationship

exists between relative density and friction angle across all the results. Notably, the slopes of these lines exhibit slight variations, potentially attributed to differences in materials and their associated normal stress.

Subsequently, an exploration into the effects of sand particle size on shear strength parameters at a constant relative density (D_r = 60%) was conducted.

The presented results, showcased in Figure 12 alongside the findings from Su et al. [24], highlight a remarkable agreement between the two datasets. This concordance underscores the precision and reliability of the laboratory data, emphasizing the consistency of the observed trends with existing research.

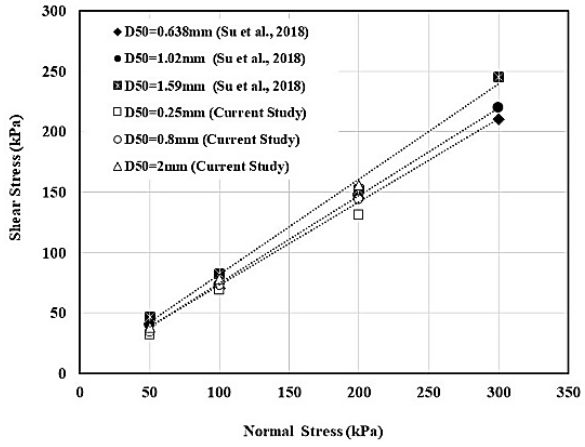

Figure 12. Direct shear strength envelopes of sand with different grain sizes (D_r = 60%).

Evidently, the augmentation in grain size is accompanied by an increase in the slope of the shear stress-normal stress graph. In simpler terms, as the size of the aggregates grows, so does the friction angle. For all three types of sand, under a constant relative density of 60%, the corresponding friction angle values stand at 33, 36, and 38 degrees.

For a comprehensive overview, Table 3 provides a breakdown of friction angle values across various relative densities and particle sizes of sand. This tabulated presentation offers a concise summary of the observed trends, highlighting the nuanced influence of particle size on the frictional characteristics of the sands at different compaction levels.

The discernible trend is clear: an increase in relative density corresponds to a higher sand friction angle. Similarly, akin results are observed with the escalation of sand particle size, where an increase in size correlates with an augmentation in the friction angle. This consistency in outcomes reinforces the influence of both relative density and particle size on the frictional characteristics of the sand, underscoring their interplay in shaping shear strength parameters.

The outcomes derived from the analysis of pure sand samples will significantly contribute to advancing our comprehension of the mechanics governing the sand-concrete interface. The following section will provide a detailed explanation of these findings, highlighting the complex interactions at the material interface.

Table 3. Values of the internal friction angle of the concrete-sand interface layer.

D_{50} (mm) / D_r (%)	30	60	90
0.25	28	33	35
0.8	32	36	38
2	35	38	41

3.2. Sand-concrete interface

The study delved into the shear behavior of the interface layer between concrete and sand, taking into account the roughness of the concrete surface (i.e., R_{max} =0, 2, 4, and 8mm), as well as the grain size and relative density of the sand.

32.1. Effects of concrete surface roughness

Figure 13 unveils the shear stress results obtained from concrete samples with varying roughness (0, 2, 4, and 8 mm), where zero roughness denotes a smooth concrete surface. These tests were conducted in the presence of coarse sand with a grain size of D_{50} = 2mm. The figure provides a visual representation of the impact of concrete surface roughness on the shear behavior of the interface layer between concrete and sand.

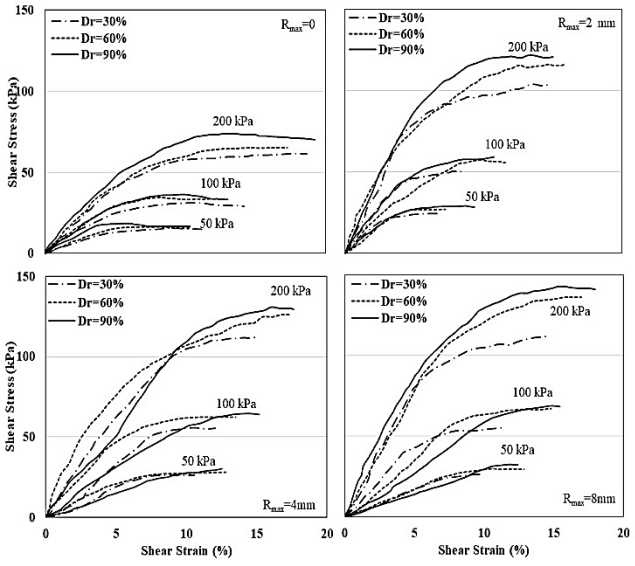

Figure 13. Effects of concrete surface roughness on the interface shear strength parameters - (Rmax = 0, 2, 4, and 8mm, D50 = 2mm, and Dr = 30, 60, and 90%).

As illustrated, a discernible trend emerges:

At a constant sand relative density, the augmentation of groove depth (concrete surface roughness) leads to an increase in shear stress at the interface. For a more detailed examination, Figure 14 showcases the maximum shear stress values, providing a nuanced insight into the intricate relationship between concrete surface roughness and the resulting shear stress at the interface. As groove depth increases, it enhances the interlocking between the sand particles and the roughened concrete surface, leading to an increase in shear strength. The application of all-around pressure further strengthens the connection between the particles and the concrete surface, resulting in a notable improvement in shear strength.

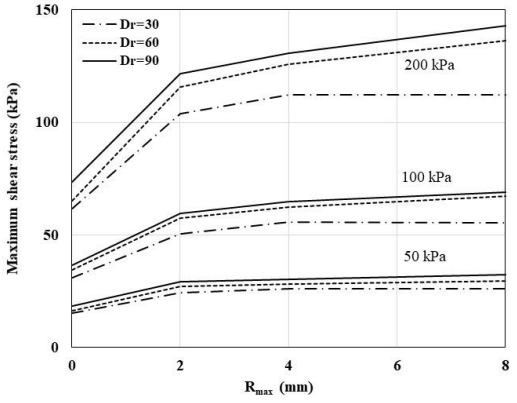

Figure 14. Maximum shear stress in different concrete surface roughness.

The observations reveal a multifaceted interplay between concrete surface roughness, relative density, and normal stress on the interface

shear strength parameters. Here are the key findings:

At a constant relative density and normal stress (e.g., D_r =60%, and σ_n = 200 kPa), an increase in groove depth from 0 to 2 mm leads to a 75% increase in maximum shear stress. Subsequent increases in R_{max} (4 and 8 mm) show a lower slope compared to R_{max} = 2mm (93% and 109%, respectively), indicating a diminishing effect on shear stress with deeper grooves. At a constant normal stress (e.g., 200 kPa) and constant roughness (e.g., R_{max} = 4 mm), an increase in relative density from 30 to 60% and 90% results in a maximum shear strength increase of approximately 12% and 16.5%, respectively, compared to Dr=30%. This underscores the significant influence of relative density on interface shear strength parameters. Concrete with a groove depth of 2 mm exhibits a substantial increase in shear strength compared to a smooth surface. However, this effect diminishes with increasing groove depth from 4 to 8 mm. While concrete roughness enhances the shear strength of the samples, the interface shear strength parameters remain consistently lower than that of pure sand. Comparisons across relative densities (30%, 60%, and 90%) reveal that the increase in relative density intensifies the effect of concrete surface roughness on interface shear strength parameters. Deeper grooves exhibit a more pronounced increase in resistance when D_r = 90% compared to D_r = 30% and 60%.

Figure 15 illustrates the interface friction angle across different relative densities and concrete surface roughness, providing a comprehensive visualization of the intricate dynamics at play. These findings collectively depict the intricate relationships governing the sand-concrete interface, shedding light on the nuanced impact of various factors on shear resistance parameters.

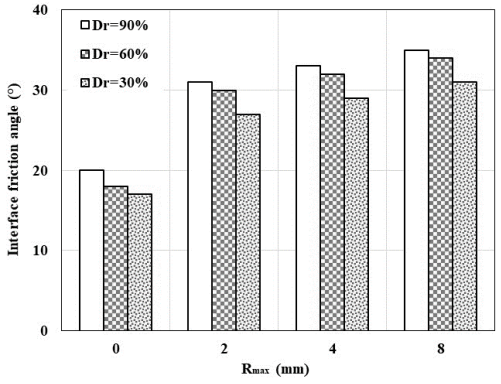

Figure 15. Interface friction angle in the different concrete surface roughness.

As observed, the augmentation in groove depth from 0 to 2 mm induces a notable rise in the interface friction angle. This observed trend persists as the depth of the groove further increases from 2 mm to 8 mm, aligning with the findings discussed earlier regarding interface shear strength parameters. Additionally, increasing the relative density from 30% to 90% at a constant groove depth result in an enhanced interface friction angle. Notably, the impact of increasing relative density from 30% to 60% has a more pronounced effect on augmenting the friction angle at the sand-concrete interface compared to the increase from 60% to 90%.

3.2.2. Effect of the sand grain size

In an effort to comprehend the influence of sand grain size on its interface shear strength parameters, a series of experiments has been undertaken. The study involves fine, medium, and coarse sand, characterized by grain sizes of D_{50} = 0.25, 0.8, and 2mm, respectively. Two distinct concrete surface roughness conditions, namely R_{max} = 0 and 2mm, are considered for each sand size. The data illustrated in Figure 16 highlights the shear stress ratio, representing the percentage increase in shear strength concerning samples with D_{50} = 0.25mm, across various sand sizes. This analysis focuses particularly on concrete surface roughness conditions of 0 and 2mm. It is important to note that the relative density of the sand in this set of experiments is maintained at 60%.

The results show that at a constant grain size and concrete roughness (e.g., D_{50} = 2mm, and R_{max} = 2mm), an increase in normal stress from 50 to 100 and 200 kPa results in a corresponding rise in the maximum shear strength ratio by approximately 45% and 47%, respectively. These findings underscore the sensitivity of interface shear strength to changes in normal stress. Furthermore, the results demonstrate that, for a specific normal stress, the interface shear strength of coarse sand surpasses that of fine and medium sand. The influence of sand particle size on results becomes more pronounced with increased normal stress.

At a constant normal stress and constant roughness (e.g., σ_n = 50 kPa and R_{max} = 0, respectively), increasing D_{50} from 0.25 mm to 2 mm leads to an 11% increase in shear stress. This highlights the impact of sand particle size on interface shear strength, with concrete surface roughness and normal stress further intensifying their effects.

Figure 17 encapsulates the direct shear strength envelopes of the concrete interface, considering different roughness conditions (R_{max} = 0 and 2mm) and varying sand grain sizes (D_{50} = 0.25, 0.8, and 2mm). This visual representation provides a holistic view of the interplay between concrete surface characteristics, sand grain sizes, and the resulting interface shear strength.

As observed, a clear correlation emerges—larger sand grains correlate with an increase in interface shear parameters, encompassing both friction angle and shear resistance. Detailed information on interface friction angles across various sand grain sizes and concrete surface roughness conditions is presented in Table 4, offering a thorough depiction of the nuanced variations in the behavior of the sand-concrete interface.

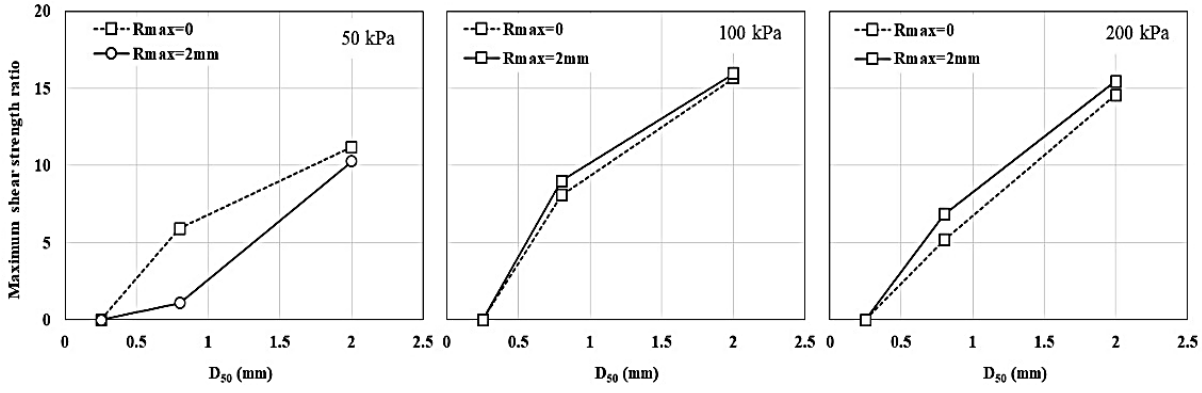

Figure 16. Maximum interface shear stress ratio with different sand grain size (Dr = 60%).

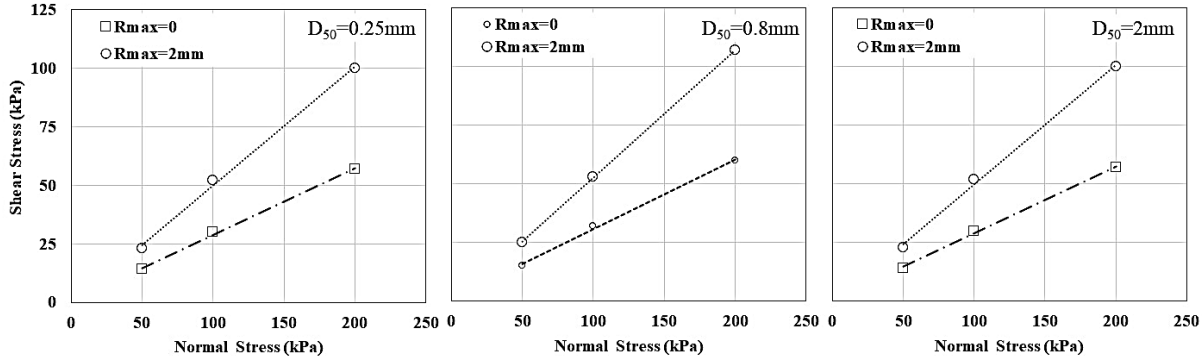

Figure 17. Direct shear strength envelopes of interface of concrete (Rmax =0 and 2mm, D50 =0.25, 0.8, and 2mm, and Dr =60%).

As observed, with a constant sand grain size (e.g., D_{50}= 0.25mm), the interface friction angle shows a significant increase of about 64% as the concrete surface roughness increases. Furthermore, when holding a consistent concrete surface roughness (e.g., R_{max} = 2mm), an increase in the sand particle size from 0.25 to 2mm leads to a corresponding 17% rise in the friction angle.

Table 4. Interface friction angle of concrete and sand.

R_{max}(mm) / D_{50}(mm)	0.25	0.8	2
0	15.6	15.8	16.5
2	25.6	27	30

4. Conclusion

This thorough investigation into the interface behavior between sand and concrete involved a nuanced examination of factors such as sand grain size, concrete surface roughness, and relative density. Employing a meticulous series of direct shear tests, we untangled the complexities influencing shear strength parameters in both pure sand and sand-concrete interfaces. The derived insights establish a sturdy groundwork for comprehending the intricate dynamics inherent in civil engineering projects, providing valuable information to inform and guide decision-making processes. The following conclusions emerge from the discerned patterns and relationships within the obtained results:

1- Our study on the influence of relative density on shear strength in pure sand reveals a significant correlation between normal stress, relative density, and shear strength parameters. Notably, an increase in mean effective size from 0.25 to 2 mm leads to an escalation in shear strength, with increments of 8% and 18% for transitions from 0.25mm to 0.8mm and 0.8mm to 2 mm, respectively. Additionally, the direct shear tests underscore the pivotal role of grain size in determining soil shear strength under varying normal stresses. The linear correlation between relative density and friction angle further emphasizes the nuanced relationship between soil compaction and frictional characteristics.

2- The findings indicate a noticeable increase in shear stress with greater groove depth, emphasizing the interplay of roughness, relative density, and normal stress. Notably, deeper grooves exhibit enhanced resistance, particularly at higher relative densities. The interface friction angle, aligns with these trends, showcasing an upward trajectory with increasing groove depth and relative density.

3- The investigation into sand grain size effects on interface shear strength provides valuable insights. Notably, larger sand grains exhibit increased shear strength ratios, outperforming fine and medium sand, particularly under higher normal stresses. The clear correlation between larger grains and elevated shear parameters, coupled with nuanced variations in friction angles, underscores the intricate dynamics governing the sand-concrete interface.

The insights derived from this study establish a strong foundation for civil engineering projects involving soil-structure interactions. These findings provide crucial information to guide decision-making processes, particularly in selecting materials and designing surface roughness profiles to enhance interface stability and strength. The results also have broader implications for projects where soil-concrete interaction is critical, such as in seismic engineering, deep foundation design, and earth-retaining structures. The study's outcomes can help refine predictive models for soil-concrete interfaces under various load conditions, leading to safer and more cost-effective designs.

Future research could investigate the effects of additional surface treatments or environmental factors—such as moisture, temperature fluctuations, or cyclic loading—on shear strength behavior at the interface. Additionally, exploring the impact of different concrete types or the role of geosynthetics in enhancing interface properties may offer valuable insights for improving performance in more complex construction environments.

References

[1] C. Du, D. Li, F. Yi, L. Wang, B. Niu, Analysis of interface mechanical properties between geotextiles and tailings during pull-out tests, PLOS ONE 17 (2022) e0276543. https://doi.org/10.1371/journal.pone.0276543.

[2] M. Maleki, H. Sereshteh, M. Mousivand, M. Bayat, An equivalent beam model for the analysis of tunnel-building interaction, Tunnelling and Underground Space Technology 26 (2011) 524–533. https://doi.org/10.1016/j.tust.2011.02.006.

[3] J. Ruiz-García, Mainshock-Aftershock Ground Motion Features and Their Influence in Building's Seismic Response, Journal of Earthquake Engineering 16 (2012) 719–737. https://doi.org/10.1080/13632469.2012.663154.

[4] A. Motallebiyan, M. Bayat, B. Nadi, Analyzing the Effects of Soil-Structure Interactions on the Static Response of Onshore Wind Turbine Foundations Using Finite Element Method, Civ. Eng. Infrastruct. J. 53 (2020). https://doi.org/10.22059/ceij.2020.281914.1586.

[5] Q. Zhang, C. Zhang, Nonlinear shear characteristics of frozen loess-concrete interface, PLOS ONE 18 (2023) e0290025. https://doi.org/10.1371/journal.pone.0290025.

[6] Influence mechanism of structure on shear mechanical deformation characteristics of loess-steel interface | PLOS ONE, (n.d.). https://journals.plos.org/plosone/article?id=10.1371/journal.pone.0263676 (accessed November 14, 2023).

[7] R.K. Rowe, S.K. Ho, Continuous Panel Reinforced Soil Walls on Rigid Foundations, Journal of Geotechnical and

Geoenvironmental Engineering 123 (1997) 912–920. https://doi.org/10.1061/(ASCE)1090-0241(1997)123:10(912).

[8] Numerical Modeling of Seismic Response of Rigid Foundation on Soft Soil | International Journal of Geomechanics | Vol 8, No 6, (n.d.). https://ascelibrary.org/doi/10.1061/%28ASCE%291532-3641%282008%298%3A6%28336%29 (accessed November 14, 2023).

[9] B.M. Das, Introduction to soil mechanics, Ames: Iowa State University Press, 1979. http://archive.org/details/introductiontoso0000dasb (accessed November 14, 2023).

[10] F. Tatsuoka, On the Angle of Interface Friction For Cohesionless Soils, Soils and Foundations 25 (1985) 135–141. https://doi.org/10.3208/sandf1972.25.4_135.

[11] Z. Wang, W. Richwien, A Study of Soil-Reinforcement Interface Friction, Journal of Geotechnical and Geoenvironmental Engineering 128 (2002) 92–94. https://doi.org/10.1061/(ASCE)1090-0241(2002)128:1(92).

[12] F. Han, E. Ganju, R. Salgado, M. Prezzi, Effects of Interface Roughness, Particle Geometry, and Gradation on the Sand–Steel Interface Friction Angle, J. Geotech. Geoenviron. Eng. 144 (2018) 04018096. https://doi.org/10.1061/(ASCE)GT.1943-5606.0001990.

[13] A.K. Janipour, M. Mousivand, M. Bayat, Study of interface shear strength between sand and concrete, Arab J Geosci 15 (2022) 172. https://doi.org/10.1007/s12517-021-09394-0.

[14] L. Hu, J. Pu, Testing and Modeling of Soil-Structure Interface, J. Geotech. Geoenviron. Eng. 130 (2004) 851–860. https://doi.org/10.1061/(ASCE)1090-0241(2004)130:8(851).

[15] T.B. Hamid, G.A. Miller, Shear strength of unsaturated soil interfaces, Can. Geotech. J. 46 (2009) 595–606. https://doi.org/10.1139/T09-002.

[16] X. Chen, J. Zhang, Y. Xiao, J. Li, Effect of roughness on shear behavior of red clay – concrete interface in large-scale direct shear tests, Can. Geotech. J. 52 (2015) 1122–1135. https://doi.org/10.1139/cgj-2014-0399.

[17] A.G. Noroozi, R. Ajalloeian, M. Bayat, Effect of FTC on the interface between soil materials and asphalt concrete using a direct shear test, Case Studies in Construction Materials 17 (2022) e01632. https://doi.org/10.1016/j.cscm.2022.e01632.

[18] A.G. Noroozi, R. Ajalloeian, M. Bayat, Experimental study of the role of interface element in earth dams with asphalt concrete core - Case study: Mijran dam, Case Studies in Construction Materials 16 (2022) e01004. https://doi.org/10.1016/j.cscm.2022.e01004.

[19] W.-Q. Feng, M. Bayat, Z. Mousavi, A.-G. Li, J.-F. Lin, Shear strength enhancement at the sand-steel interface: A pioneering approach with Polyurethane Foam Adhesive (PFA), Construction and Building Materials 429 (2024) 136297.

[20] W.-Q. Feng, Z. Mousavi, M. Farhadi, M. Bayat, M.M. Ettefagh, S. Varahram, M.H. Sadeghi, A hybrid wavelet-deep learning approach for vibration-based damage detection in monopile offshore structures considering soil interaction, J Civil Struct Health Monit (2024). https://doi.org/10.1007/s13349-024-00876-9.

[21] H. Kishida, M. Uesugi, Tests of the interface between sand and steel in the simple shear apparatus, Géotechnique 37 (1987) 45–52. https://doi.org/10.1680/geot.1987.37.1.45.

[22] A.M. Gokhale, E.E. Underwood, A general method for estimation of fracture surface roughness: Part I. Theoretical aspects, Metall Trans A 21 (1990) 1193–1199. https://doi.org/10.1007/BF02698249.

[23] A. Ahmadi, M.A. Nozari, M. Bayat, E. Delavari, Investigating Calcareous and Silica Sand Behavior at Material Interfaces: A Comprehensive Study, Studia Geotechnica et Mechanica 0 (2024). https://doi.org/10.2478/sgem-2024-0023.

[24] L.-J. Su, W.-H. Zhou, W.-B. Chen, X. Jie, Effects of relative roughness and mean particle size on the shear strength of sand-steel interface, Measurement 122 (2018) 339–346. https://doi.org/10.1016/j.measurement.2018.03.003.

[25] H. Haeri, V. Sarfarazi, Z. Zhu, M.F. Marji, A. Masoumi, Investigation of shear behavior of soil-concrete interface, Smart Structures and Systems 23 (2019) 81–90.

[26] Y.-B. Wang, C. Zhao, Y. Wu, Study on the effects of grouting and roughness on the shear behavior of cohesive soil–concrete interfaces, Materials 13 (2020) 3043.

[27] C. Kim, L. Chen, H. Wang, H. Castaneda, Global and local parameters for characterizing and modeling external corrosion in underground coated steel pipelines: A review of critical factors, Journal of Pipeline Science and Engineering 1 (2021) 17–35.

[28] M. Yang, S. Kainuma, Investigation of steel corrosion near the air–liquid interface in NaCl solution and soil environment, Corrosion Engineering, Science and Technology 56 (2021) 690–702. https://doi.org/10.1080/1478422X.2021.1943818.

[29] Y. Wang, W. Wang, J. Huang, L. Luo, Effect of corrosion on soil-structure interfacial shearing property and bearing capacity of steel foundation in submarine soil environment, Computers and Geotechnics 156 (2023) 105269.

[30] E. Ravera, M. Sutman, L. Laloui, Cyclic thermomechanical response of fine-grained soil–concrete interface for energy piles applications, Can. Geotech. J. 58 (2021) 1216–1230. https://doi.org/10.1139/cgj-2020-0437.

[31] M. Uesugi, H. Kishida, Frictional Resistance at Yield between Dry Sand and Mild Steel, Soils and Foundations 26 (1986) 139–149. https://doi.org/10.3208/sandf1972.26.4_139.

[32] G.A. Athanasopoulos, Effect of particle size on the mechanical behaviour of sand-geotextile composites, Geotextiles and Geomembranes 12 (1993) 255–273.

[33] H. Peng-Fei, M. Yan-Hu, M. Wei, Y.-T. Huang, D. Jian-Hua, Testing and modeling of frozen clay–concrete interface behavior based on large-scale shear tests, Advances in Climate Change Research 12 (2021) 83–94.

[34] L. Chen, J. He, B. Yao, C. Lei, Z. Zhang, Influence of the Initial Relative Density on the Drained Strength Properties of Soils Subjected to Internal Erosion, Soil Mech Found Eng 56 (2019) 273–279. https://doi.org/10.1007/s11204-019-09602-w.

[35] S.V. Maghvan, R. Imam, J.S. McCartney, Relative density effects on the bearing capacity of unsaturated sand, Soils and Foundations 59 (2019) 1280–1291.